ELSEVIER

International Journal of Heat and Fluid Flow 21 (2000) 381–387

International Journal of HEAT AND FLUID FLOW

www.elsevier.com/locate/ijhff

Test of an Eulerian–Lagrangian simulation of wall heat transfer in a gas-solid pipe flow

P. Boulet *, S. Moissette, R. Andreux, B. Oesterlé

Laboratoire Universitaire de Mécanique et Energétique de Nancy (L.U.M.E.N.), E.S.S.T.I.N. – Université Henri Poincaré, Nancy 1, 2 rue Jean Lamour, F-54500 Vandoeuvre, France

Received 3 September 1999; accepted 1 February 2000

Abstract

An Eulerian–Lagrangian model is proposed to numerically predict the heat transfer between a vertical pipe wall and a turbulent gas-solid suspension. The whole problem lies in the combined solution of mass, momentum, and energy equations written for each phase. Closure equations devoted to turbulence and heat transfer simulation are also needed for the continuous phase. This problem is treated using a k–ε model and a turbulent Prandtl number model for the gaseous phase. The coupling terms standing for the fluid–particle interactions are taken into account. The simulation of the dispersed phase dynamics is addressed using a Lagrangian model, taking the particle–wall and particle–particle interactions into account. Additionally, the temperature of each particle is tracked using a model for the convective heat exchange between the two phases. The accuracy of the thermal and dynamic solutions has been tested for particles of diameter 200 and 500 μm, and for a wide range of loading ratios (0–20). Corresponding velocity and turbulent kinetic energy profiles are presented for the dynamic modelling validation, while Nusselt numbers are calculated for the study of the thermal problem.

Keywords: Eulerian–Lagrangian; Gas-particle flow; Heat transfer

Notation

A_p	surface area of a particle
C_D	drag coefficient
C_p	specific heat
d_p	particle diameter
g	gravitational acceleration
h_p	heat transfer coefficient around particles
k	turbulent kinetic energy
m	solid loading ratio
n_p	number of particles (/m^3)
Nu	Nusselt number
Nu_L	asymptotic Nusselt number
Nu_p	particle Nusselt number
Nu_0	pure air Nusselt number
Pr	Prandtl number
Pr_t	turbulent Prandtl number
Q_W	wall heat flux
Re	pipe flow Reynolds number
Re_p	particle Reynolds number
Re_t	turbulent Reynolds number
r	radial co-ordinate
R	pipe radius
S_{pk}	kinetic energy source term
$S_{p\varepsilon}$	dissipation rate source term
S_{pu}	momentum source term
S_{pT}	heat source term due to fluid particle exchange
T	temperature
T_m	bulk average temperature
u^+	fluid velocity in wall unit
u_c	velocity at the pipe centre
u_z	fluid velocity
u_τ	friction velocity
v_z	particle velocity
V_p	volume of a particle
y^+	wall distance in wall unit
z	axial co-ordinate

Greeks

α	solid volume fraction
ε	dissipation rate of turbulent kinetic energy
ε_t	thermal eddy diffusivity
κ	Von Karman constant
λ_f	fluid thermal conductivity
ν	laminar cinematic viscosity
ν_t	eddy viscosity
ρ	density
τ_p	particle relaxation time

Subscripts and superscripts

f	fluid property
p	particle property

* Corresponding author.
E-mail address: boulet@esstin.u-nancy.fr (P. Boulet).

0142-727X/00/$ - see front matter
PII: S0142-727X(00)00024-2

t turbulent quantity
W property at the wall
– averaged quantity
′ fluctuating quantity

1. Introduction

Addition of particles in a gas turbulently flowing in a pipe is well known to have an influence on the dynamic flow characteristics and on the heat transfer between the wall and the suspension. Among the factors affecting these phenomena, the loading ratio, the particle characteristics, the inter-particle collisions, the particle–turbulence interactions as well as the flow regime have been identified. At low loading ratios for example, it has been experimentally noticed that the turbulent intensity tends to decrease for small particles, while it tends to increase for large particles. Simultaneously, the heat transfer between the wall and the suspension seems to decrease at low loading ratios and to increase at higher loading ratios. This last phenomenon has been especially observed through experimental data by Depew and Farbar (1963) and Jepson et al. (1963), among others, who reported measurements of the suspension Nusselt number as a function of the loading ratio for several kinds of particles.

The aim of this paper is to present a numerical simulation of a turbulent gas-solid flow in a vertical pipe, heated by a constant wall heat flux. The injected particles are assumed to be spherical with a diameter of 200 μm or 500 μm. The predictions of the velocity and temperature fields are based on an Eulerian–Lagrangian approach. In fact, the work is in keeping with various studies which aim to simulate these kinds of flows more and more accurately by means of Eulerian or Lagrangian modelling. For example, in the two-fluid approach suggested by Han et al. (1991), the turbulent Prandtl number is expressed as a function of the solid-to-fluid heat capacity ratio and the ratio of the turbulent time scale to the particle thermal relaxation time. Treating a similar problem, Avila and Cervantes (1995) have used an Eulerian–Lagrangian approach based on a standard k–ε model and on an enthalpy balance for the continuous phase, while the Lagrangian–Stochastic deterministic (LSD) model was used to predict the particulate phase motion, inter–particle collisions and wall–particle interactions being neglected, however. Boulet et al. (1998) have recently combined the two approaches, using a two-fluid model in order to simulate the dynamic and thermal characteristics, closure being achieved on the basis of Lagrangian simulation results.

In the present Eulerian–Lagrangian formulation, one of the objectives was to bring special care to the interactions between the turbulence and the particles. The formulation thus takes into account the appropriate coupling terms in the various equations. The fluid flow is predicted by means of a standard k–ε model, whereas the thermal problem is solved using a turbulent Prandtl number expression by Kays (1994) for the closure. This formulation allows the large increase of the turbulent Prandtl number in the near-wall region to be taken into account. The dynamic features of the particle flow are predicted through an improved version of the Lagrangian simulation presented by Oesterlé and Petitjean (1993), where particular attention is paid to the effects of collisions undergone by particles. For the present purpose, it has been supplemented by temperature tracking based on the energy balance of each particle along its trajectory.

In the following sections, the needed assumptions and the mathematical formulation of the problem are first presented. Then, the numerical procedure is described, including the axial and radial grid definition. Finally, after comparing predictions concerning the fluid and the particle dynamics to experimental data by Tsuji et al. (1984), the numerical heat transfer results are validated against the experimental data by Depew and Farbar (1963) and Jepson et al. (1963).

2. Formulation

2.1. Dynamic problem

The basic assumptions used in the mathematical formulation of the dynamic models are the following:

1. the gas is incompressible;
2. the gas-solid suspension is flowing upward in a vertical pipe;
3. the flow is quasi-developed in the axial direction (convection terms being neglected and velocity profiles being only altered due to fluid–particle interactions);
4. particles are solid, spherical, with a constant diameter.

Under above conditions, the k–ε model may be written as follows:

Momentum equation:

$$-(1-\overline{\alpha})\frac{\mathrm{d}\overline{P}}{\mathrm{d}z}-\rho_{\mathrm{f}}(1-\overline{\alpha})g+\frac{1}{r}\frac{\mathrm{d}}{\mathrm{d}r}\left[r\rho_{\mathrm{f}}(1-\overline{\alpha})\,\nu_{\mathrm{t}}\frac{\mathrm{d}\overline{u_z}}{\mathrm{d}r}\right]+\overline{S_{\mathrm{p}u}}=0. \tag{1}$$

Turbulent energy equation:

$$\frac{1}{r}\frac{\mathrm{d}}{\mathrm{d}r}\left[r(1-\overline{\alpha})\frac{\nu_{\mathrm{t}}}{\sigma_k}\frac{\mathrm{d}\overline{k}}{\mathrm{d}r}\right]+(1-\overline{\alpha})\nu_{\mathrm{t}}\left[\frac{\mathrm{d}\overline{u_z}}{\mathrm{d}r}\right]^2-(1-\overline{\alpha})\overline{\varepsilon}+\overline{S_{\mathrm{p}k}}=0. \tag{2}$$

Dissipation rate equation:

$$\frac{1}{r}\frac{\mathrm{d}}{\mathrm{d}r}\left[r(1-\overline{\alpha})\frac{\nu_{\mathrm{t}}}{\sigma_\varepsilon}\frac{\mathrm{d}\overline{\varepsilon}}{\mathrm{d}r}\right]+C_1(1-\overline{\alpha})\,\nu_{\mathrm{t}}\frac{\overline{\varepsilon}}{\overline{k}}\left[\frac{\mathrm{d}\overline{u_z}}{\mathrm{d}r}\right]^2-C_2(1-\overline{\alpha})\frac{\overline{\varepsilon}^2}{\overline{k}}+\overline{S_{\mathrm{p}\varepsilon}}=0. \tag{3}$$

Closure equation:

$$\nu_{\mathrm{t}}=C_\mu\frac{\overline{k}^2}{\overline{\varepsilon}}. \tag{4}$$

Commonly adopted values are taken for the model constants C_μ, C_1, C_2, σ_k and σ_ε. The coupling terms $\overline{S_{\mathrm{p}u}}$, $\overline{S_{\mathrm{p}k}}$ and $\overline{S_{\mathrm{p}\varepsilon}}$ are given by:

$$\overline{S_{\mathrm{p}u}}=\frac{\alpha\rho_{\mathrm{p}}}{\tau_{\mathrm{p}}}(\overline{v_z}-\overline{u_z}), \tag{5}$$

where

$$\tau_{\mathrm{p}}=\frac{4}{3}\frac{\rho_{\mathrm{p}}d_{\mathrm{p}}}{\rho_{\mathrm{f}}C_{\mathrm{D}}|\overline{v_z}-\overline{u_z}|}$$

is the particle dynamic relaxation time.

$$\overline{S_{\mathrm{p}k}}\approx\overline{S'_{\mathrm{p}u}u'}=\overline{S_{\mathrm{p}u}u_z}-\overline{S_{\mathrm{p}u}}\,\overline{u_z} \tag{6}$$

$$\overline{S_{\mathrm{p}\varepsilon}}=C\frac{\varepsilon}{k}\overline{S_{\mathrm{p}k}} \tag{7}$$

as proposed by Berlemont et al. (1997) with $C=1,9$.

It must be noticed that this formulation of the source terms for fluid turbulent kinetic energy and dissipation rate does not allow the turbulence generation in particle wakes to be taken into account. As shown by Crowe and Gillandt (1998), who derived an equation for the fluid turbulent kinetic energy which is in accordance with the previously reported formulation by Hwang and Shen (1993), the source

term expression (6) is faulty in the limiting case of particles artificially fixed in position in a gas flow. Unfortunately, in the above-mentioned references, there is no available model for the corresponding dissipation rate, which in this case should include the dissipation in particle wakes. In the presently used formulation by Eqs. (6) and (7), it is implicitly assumed that the turbulence production and dissipation are in equilibrium in the particle wake, an assumption which has be proven to yield satisfactory results provided that the gas-particle flow is far enough from the asymptotic case considered by Crowe and Gillandt (1998). This is the reason why the present model of coupling terms remains a commonly used tool, keeping in mind that it is not capable of predicting some observed turbulence augmentation in gas-solid flows with very large particles, as reported by Tsuji et al. (1984) for example.

The simulation of the dispersed phase dynamics follows the Lagrangian code presented by Oesterlé and Petitjean (1993), which is based on a probabilistic technique to treat the inter-particle collisions. The effect of turbulent fluctuations is simulated by an eddy interaction model.

2.2. Thermal formulation

The basic assumptions used in the mathematical formulation of the thermal problem, allowing the study of the heat transfer between the heated pipe and the suspension, are the following ones:

1. each particle has a uniform temperature and constant characteristics;
2. the heat transfer by conduction due to particle-particle interactions and wall-particles interactions is negligible;
3. the heat flux at the pipe wall is uniform;
4. axial heat transfer is negligible compared to radial one;
5. temperatures considered are sufficiently low to neglect the radiative transfer.

Under above conditions, the thermal problem for the fluid flow is modelled as follows:

Energy balance:

$$(1-\overline{\alpha})\rho_f C_{pf}\overline{u}_z\frac{\partial\overline{T_f}}{\partial z}=\frac{1}{r}\frac{\partial}{\partial r}\left(r(1-\overline{\alpha})(\lambda_f+\rho_f C_{pf}\varepsilon_t)\frac{\partial\overline{T_f}}{\partial r}\right)+\overline{S_{pT}}. \tag{8}$$

Closure relation:

$$\varepsilon_t=\nu_t/Pr_t. \tag{9}$$

The expression of the turbulent Prandtl number Pr_t is given by Kays (1994) as:

$$Pr_t=\{0.5882+0.228(\nu_t/\nu)-0.0441(\nu_t/\nu)^2[1-\exp((-5.165/\nu_t)\nu)]\}^{-1}. \tag{10}$$

The coupling term $\overline{S_{pT}}$ which represents the heat exchange between the particulate phase and the continuous phase, is given by:

$$\overline{S_{pT}}=\frac{6\alpha h_p}{d_p}\left(\overline{T_p}-\overline{T_f}\right), \tag{11}$$

where h_p, the heat transfer coefficient characterising the convection around particles, is deduced from a corresponding particle Nusselt number: $Nu_p=h_p d_p/\lambda_f$ defined as in Avila and Cervantes (1995):

- $0\leqslant Re_p\leqslant 1$ $\quad Nu_p=1+(1+Re_p Pr)^{0.333}$
- $1\leqslant Re_p\leqslant 100$ $\quad Nu_p=Re_p^{0.41}\left(1+\frac{1}{Re_p Pr}\right)^{0.333}Pr^{0.333}+1$
- $100\leqslant Re_p\leqslant 2000$ $\quad Nu_p=0.752\,Re_p^{0.472}\left(1+\frac{1}{Re_p Pr}\right)^{0.333}Pr^{0.333}+1$

(12)

The temperature of each particle is calculated along its trajectory, by solving the following energy balance:

$$\rho_p V_p C_p\frac{dT_p}{dt}=h_p A_p(\overline{T_f}-T_p). \tag{13}$$

Finally, the associated boundary conditions are:

At the pipe inlet: $T_f=T_p=T_0$;

at the axis: $\partial\overline{Tf}/\partial r\big|_{r=0}=0$

At the wall: $Q_W=-\lambda_f\partial\overline{T_f}/\partial r\big|_{r=R}$. (14)

3. Numerical procedure

Equations are numerically solved using a finite-difference scheme. The geometry of the here-studied pipe may be divided into two parts, the adiabatic inlet section and the heated section. At the end of the first part the flow is assumed to be dynamically fully developed. We are primary interested in the second section, where the wall is heated, thus leading to a thermally developing flow. This arrangement is similar to the classical set-up used in the above-mentioned experimental works.

3.1. Numerical grid

In order to accurately handle the heat transfer problem, it is necessary that the mesh width be small enough near the wall. A logarithmic scheme as proposed by Wassel and Edwards (1976) is used for the radial co-ordinate definition:

$$r(i)=R\left(1-\frac{1}{\kappa Re_t}\left[\exp\left(\frac{i}{n_r}\ln(1+\kappa\,Re_t)\right)-1\right]\right) \tag{15}$$

with $i=[1;\ldots;n_r]$, where n_r is the number of nodes in the radial direction, κ is the Von Karman constant and Re_t denotes a turbulent Reynolds number defined as $Re_t=u_\tau R/\nu$, $u_\tau$being the friction velocity. For the axial co-ordinate, the following grid definition, suggested by Azad and Modest (1981), is adopted in the heated section:

$$z(i)=\frac{\exp[(i/n_z)\ln((cL/R)+1)]-1}{c/R} \tag{16}$$

with $i=[1;\ldots;n_z]$, where n_z is the number of nodes in the axial direction, c is a constant and L designates the heated pipe length. Numerical calculations have been carried out using the above-described co-ordinates, with $n_r=50$, $n_z=10$, $c=10$. Such a low number of grid nodes in the axial direction was chosen in order to reduce the storage needs for the Lagrangian simulation, after comparison through Eulerian computation (Boulet et al., 1998) has shown no significant difference between $n_z=10$ and $n_z=100$.

As the fluid phase dynamics is only solved in the core region (between the pipe centre and a node located at $y^+=30$) using the above-presented k–ε model, some further dynamic data are needed in the near wall region, in order that the heat transfer problem may be treated very close to the wall. This difficulty is surmounted by using an interpolation scheme between the wall and the calculated values at $y^+=30$. However, instead of applying a simple interpolation to calculate the velocity, the

standard three-layer formulation has been preferred in the near-wall region. Similarly, the eddy viscosity close to the wall is calculated using the Van Driest formula as modified in Azad and Modest (1981):

$$\nu_t = \frac{\kappa}{10}\nu\left[\exp(\kappa u^+) - 1 - \kappa u^+ - \frac{(\kappa u^+)^2}{2!} - \frac{(\kappa u^+)^3}{3!}\right] \quad \text{for } y^+ < 40. \tag{17}$$

3.2. Numerical technique

Equations are numerically handled using a finite difference technique. An iterative numerical method is applied in order to allow all the coupling terms between the two phases to be taken into account. Numerical tests have been carried out in order to give the optimum scheme to obtain the convergence of the two-way approach.

The dynamic problem is finally treated according to the following steps:

1. seeking for a solution to the continuous phase equations starting with simple particle phase characteristics (constant velocity and concentration);
2. tracking of particles injected in the corresponding air flow;
3. solution of the continuous phase loaded with particles with properties calculated above;
4. successive treatment of previous steps until satisfactory convergence criteria are obtained.

In the hereafter presented examples, three successive loops have been carried out between the Eulerian and the Lagrangian simulations, 5,000–15,000 particle trajectories being calculated in each Lagrangian simulation. Any additional coupling iteration did not introduce significant alteration of the dynamic results in case of moderate loading ratios (less than 3.6).

After computing the two-phase flow dynamics, the thermal problem in the heated part of the pipe is dealt with, repeating the two following steps successively:

1. seeking for a solution to the energy balance on the continuous phase;
2. calculation of the particle temperature along their trajectories.

In the examples presented in the following section, two loops between Eulerian and Lagrangian treatments were found to be sufficient to yield stable numerical results for the thermal problem. However, more coupling-iterations would be needed for larger loading ratios.

4. Numerical validation

4.1. Dynamic characteristics

First validation tests have been carried out for the dynamic characteristics, numerical results being compared to the experimental data of Tsuji et al. (1984). Velocity and streamwise turbulent intensity profiles are presented in Figs. 1–4. The studied cases correspond to an air flow loaded with particles with a density of 1020 kg/m^3 and a diameter of 500 μm. The pipe diameter is 3.05 cm.

Velocity profiles are plotted in Fig. 1 for a loading ratio of 2 and a mean fluid velocity of 8 m/s. Results are normalised, dividing by the fluid velocity at the pipe centre. The same presentation is kept in Fig. 2, for a larger loading ratio ($m = 3.6$) and a similar mean fluid velocity of 7.89 m/s. Particle velocity profiles are especially well reproduced thanks to the use of a realistic virtual wall model and inelastic bouncing

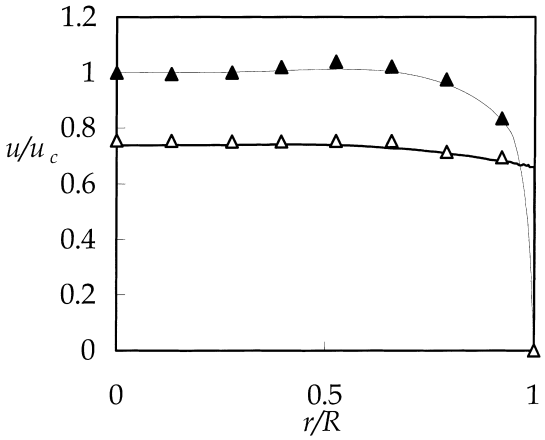

Fig. 1. Velocity profiles (the thin line stands for the fluid and the heavy line for the particles). Comparison with Tsuji's experiments (symbols) ($Re \approx 16{,}000$; $m = 2.0$; $d_p = 500$ μm).

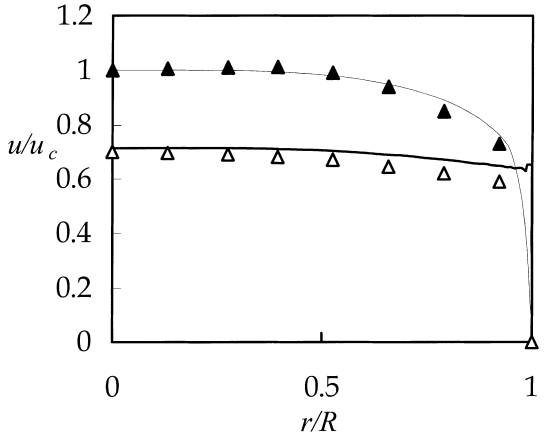

Fig. 2. Velocity profiles (the thin line stands for the fluid and the heavy line for the particles). Comparison with Tsuji's experiments (symbols) ($Re \approx 16{,}000$; $m = 3.6$; $d_p = 500$ μm).

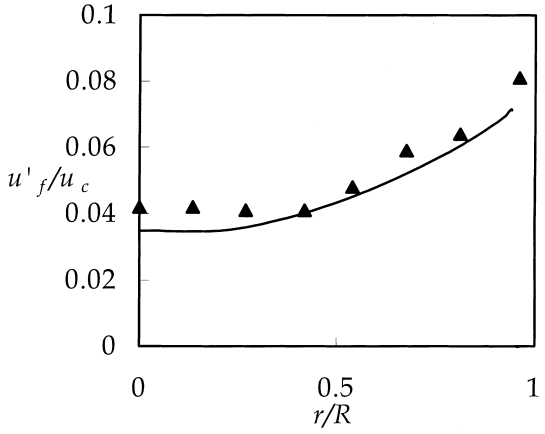

Fig. 3. Streamwise fluid r.m.s. velocity profiles. Comparison with Tsuji's experiments (symbols) ($Re \approx 22{,}000$; $m = 1.3$; $d_p = 500$ μm).

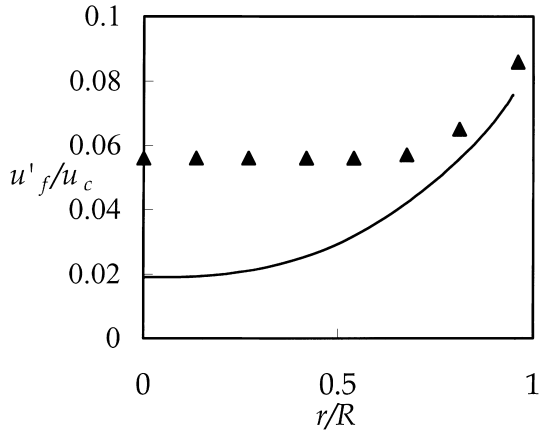

Fig. 4. Streamwise fluid rms velocity profiles. Comparison with Tsuji's experiments (symbols) ($Re \approx 22{,}000$; $m = 3.4$; $d_p = 500$ μm).

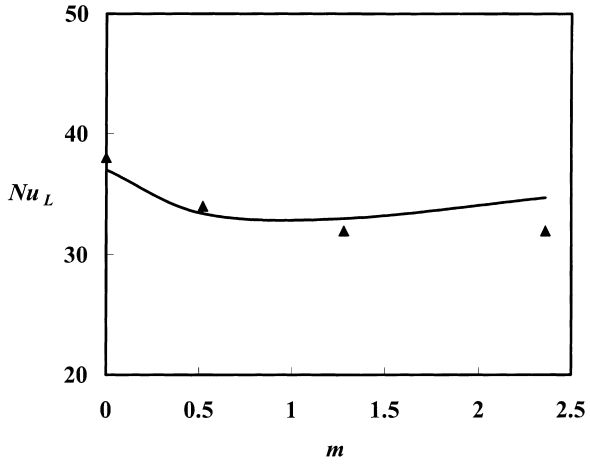

Fig. 5. Nusselt number as a function of the loading ratio. Comparison with Depew and Farbar's experiments (symbols) ($Re \approx 13{,}500$; $d_p = 200$ μm).

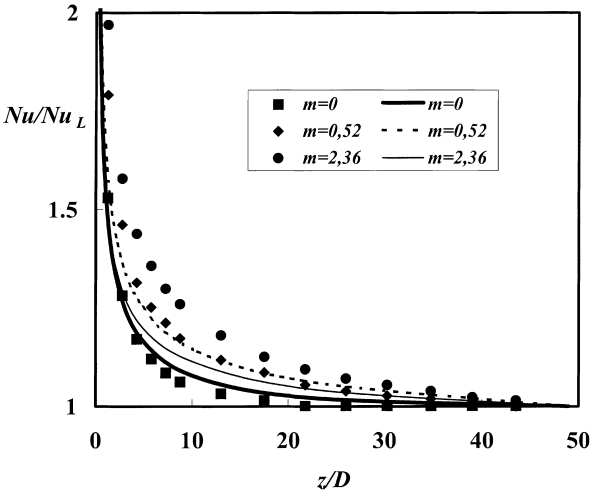

Fig. 6. Nusselt number as a function of axial position. Comparison with Depew and Farbar's experiments (symbols) ($Re \approx 13{,}500$; $d_p = 200$ μm).

conditions. One may also notice that velocity results are still very good at larger loading ratio, even for the fluid velocity (Fig. 2).

Figs. 3 and 4 are devoted to axial fluctuating velocity results, calculated in similar conditions. Particles are injected in an air flow with a mean velocity of 10.8 m/s. The loading ratio is 1.3 for Fig. 3 and 3.4 for Fig. 4. Results are good at low loading ratio (Fig. 3), whereas inaccuracies appear when more particles are injected (Fig. 4). Considering the experimental data by Tsuji et al. (1984), the fluid rms velocity should increase at the pipe centre. On the contrary, numerical results show a decrease. It seems that the present formulation of the source terms, simulating the fluid turbulence alteration due to particles, has to be improved, keeping in mind the above-mentioned limitations for Eqs. (6) and (7). Both dissipation or production of turbulence of the carrier fluid may arise, due to inter-phase exchanges, in two-phase flows. Here, production is not obtained.

More tests should also be carried out in order to improve the present simple k–ε model. In particular, the turbulence anisotropy is not taken into account. Multiple time scale models should be also used, since their ability to simulate turbulence alteration has been proved by Sato and Hishida (1996). Finally, the effects of the concentration distribution should be studied, considering its influence on the inter-particle collisions, which are expected to significantly affect the particle dispersion, thus influencing the fluid dynamics through coupling terms.

4.2. Thermal results

The thermal problem solution has been tested by means of comparisons with data by Depew and Farbar (1963) and Jepson et al. (1963). Suspension Nusselt numbers have been calculated using the following definition:

$$Nu = \frac{2RQ_W}{\lambda_f(T_W - T_m)}. \tag{18}$$

T_W and T_m being the wall temperature and the bulk average temperature, respectively.

Figs. 5 and 6 illustrate the comparison with the experiments by Depew and Farbar, who used 200 μm spherical glass beads. In Fig. 5, the Nusselt number at the end of the pipe, where the flow is fully developed, is presented as a function of the loading ratio. Agreement is good, but it must be noticed that the corresponding loading ratios are relatively small. Some decrease in the Nusselt number is first observed, then the numerical results indicate that Nu_L increases with increasing loading ratio.

In Fig. 6, local Nusselt numbers are plotted as a function of the axial location along the pipe, for several loading ratios. Qualitative agreement is obtained, showing the ability of the simulation to reproduce the thermal entry length increase due to the presence of particles. Results are even very good for $m = 0.52$. Unfortunately, predictions become inaccurate for the largest loading ratio, again indicating the limitations of the present numerical code, as stated above in the section devoted to the dynamic solution validation.

Fig. 7 presents similar tests performed in a case experimentally studied by Jepson et al. (1963). Sand particles with the same diameter (200 μm) were injected in an air flow. Comparisons are performed for the asymptotic Nusselt numbers, which are referred to the corresponding pure air flow Nusselt number. In agreement with previous observations, the general variations are qualitatively obtained, but results become inaccurate for loading ratios exceeding about 5. One may notice that for very large values of m, coupling effects between

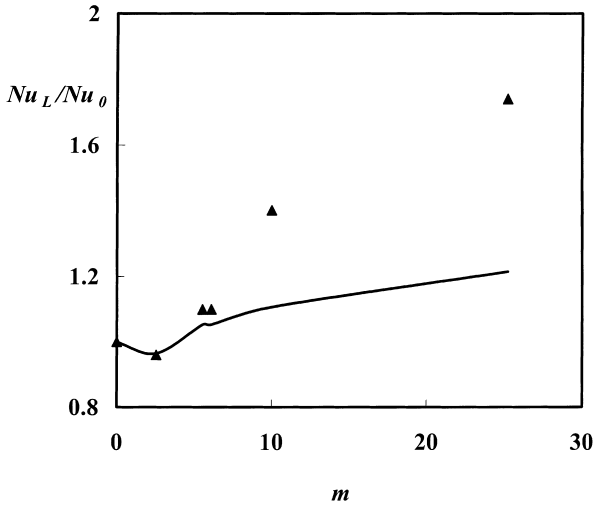

Fig. 7. Nusselt number as a function of loading ratio. Comparison with Jepson et al. experiments (symbols) ($Re \approx 23{,}000$; $d_p = 200$ μm).

the two phases are supposed to be very strong. Numerical tests are therefore currently performed about the influence of the number of tracked particle and the number of iterations between Eulerian and Lagrangian models, in order to improve the results.

Further computations have been performed for larger particles, with a diameter of 500 μm. Figs. 8 and 9 present the corresponding results, as compared to experimental data by Jepson et al. (1963), for respective Reynolds number equal to 30,400 and 46,000. As can be seen, the agreement is good for such larger particles, in this range of loading ratio ($m < 8$). The decrease in the Nusselt number, for low loading ratio, is stronger than previously seen for smaller particles. On the contrary, the increase, observed when more particles are injected, is weaker. All those phenomena due to particle effects on dynamic and thermal behavior of the suspension are well simulated numerically.

Considering the first tests performed using the present simulation, a qualitative description of the dynamic and thermal behaviour of the suspension has been obtained. However, the agreement between numerical results and

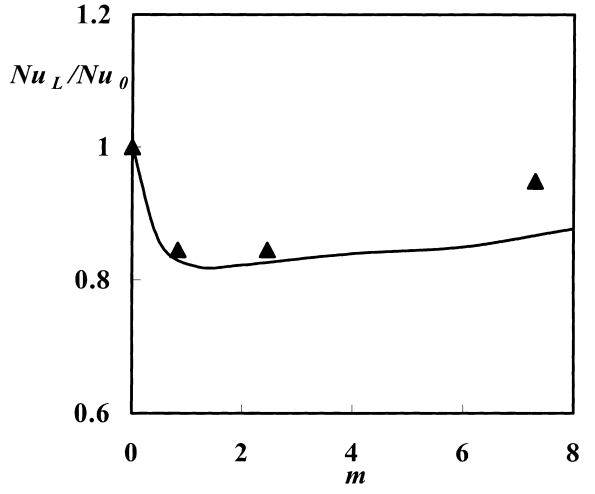

Fig. 8. Nusselt number as a function of loading ratio. Comparison with Jepson et al. experiments (symbols) ($Re \approx 30{,}400$; $d_p = 500$ μm).

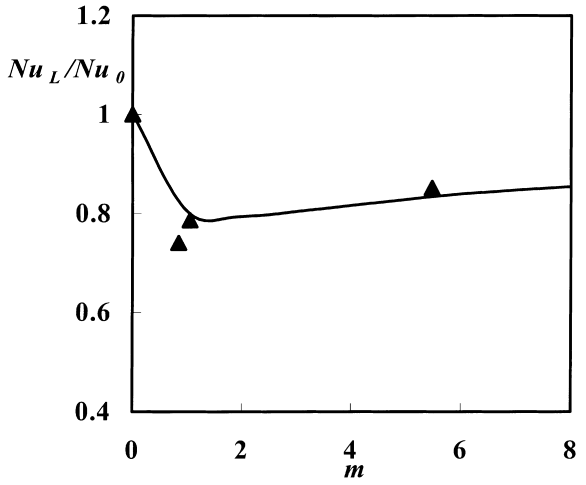

Fig. 9. Nusselt number as a function of loading ratio. Comparison with Jepson et al. experiments (symbols) ($Re \approx 46{,}000$; $d_p = 500$ μm).

experimental ones has not been found satisfactory at high loading ratio. This corresponds to flows where turbulence is significantly modified by particles. We therefore consider that this phenomenon is still misrepresented by our simulation at this moment, as previously noticed. Some further investigations must be carried out in this field. Moreover, the closure equations used in the present model are not satisfactory, since the turbulence anisotropy and the particle influence on the fluid phase turbulent Prandtl number are not yet taken into account. These will also be two major investigation subjects to be developed soon. Finally, more tests will be performed for various particle diameter, including very small ones, for which dispersion phenomena are strongly affecting the particle trajectories.

5. Conclusion

An Eulerian–Lagrangian model has been presented in order to predict the heat transfer between a turbulently flowing gas-solid suspension and a vertical pipe with a uniformly heated wall. A k–ε model combined with a complete particle tracking has been used, including coupling terms to simulate the fluid-particle interactions.

Although the presented preliminary tests indicate encouraging results, the model becomes unsatisfactory as loading ratio rises. Further study is now necessary in order to extend the validity range of the code to higher loading ratios. Subsequent investigations will be carried out, particularly in order to improve the formulation of the closure equations and the coupling terms used for the continuous phase.

References

Avila, R., Cervantes, J., 1995. Analysis of heat transfer coefficient in a turbulent particle pipe flow. Int. J. Heat Mass Transfer 38 (11), 1923.

Azad, F.H., Modest, M.F., 1981. Combined radiation and convection in absorbing emitting and anisotropically scattering gas-particulate turbulent flow. Int. J. Heat Mass Transfer 24 (10), 1681.

Berlemont, A., Desjonqueres, P., Cabot, M.S. 1997. Turbulent modification in a particle laden wall jet. ASME FEDSM' 97, Paper 97-3577.

Boulet, P., Oesterlé, B., Tanière, A. 1998. Two-fluid computation of particle effects on fluid dynamics and heat transfer in a gas-solid pipe flow. ICMF'98, P613, Lyon, France.

Crowe, C.T., Gillandt, I. 1998. Turbulence modulation of fluid-particle flows. A basic approach. ICMF'98, Lyon, France.

Depew, C.A., Farbar, L., 1963. Heat transfer to pneumatically conveyed glass particles of fixed size. Trans. ASME, J. Heat Transfer C 85, 164.

Han, K.S., Sung, H.J., Chung, M.K., 1991. Analysis of heat transfer in pipe carrying two-phase gas-particle suspension. Int. J. Heat Mass Transfer 34 (1), 69.

Hwang, G.J., Shen, H.H., 1993. Fluctuation energy equations for turbulent fluid-solid flows. Int. J. Multiphase flow 19 (5), 887.

Jepson, G., Poll, A., Smith, W., 1963. Heat transfer from gas to wall in a gas-solids transport line. Trans. Instn. Chem. Engrs. 41, 207.

Kays, W.M., 1994. Turbulent Prandtl number – Where are we?. Trans. ASME 116, 284.

Oesterlé, B., Petitjean, A., 1993. Simulation of particle to particle interactions in gas-solid flows. Int. J. Multiphase flow 19 (1), 199.

Sato, Y., Hishida, K., 1996. Transport process of turbulence energy in particle-laden turbulent flow. Int. J. Heat and Fluid Flow 17, 202.

Tsuji, Y., Morikawa, Y., Shiomi, H., 1984. LDV measurements of an air-solid two-phase flow in a vertical pipe. J. Fluid Mech. 139, 417.

Wassel, A.T., Edwards, D.K. 1976. Molecular gas radiation in a laminar or turbulent pipe flow. J. Heat transfer Paper 76-HT-Q.